Journal of Power Sources 183 (2008) 447–453

Contents lists available at ScienceDirect

Journal of Power Sources

journal homepage: www.elsevier.com/locate/jpowsour

Synthesis and characterization of cross-linked quaternized poly(vinyl alcohol)/chitosan composite anion exchange membranes for fuel cells

Ying Xiong, Qing Lin Liu*, Qiu Gen Zhang, Ai Mei Zhu

Department of Chemical & Biochemical Engineering, The College of Chemistry and Chemical Engineering, Xiamen University, Xiamen 361005, China

ARTICLE INFO

Article history:
Received 21 April 2008
Received in revised form 31 May 2008
Accepted 4 June 2008
Available online 8 June 2008

Keywords:
Quaternized polyvinyl alcohol
Quaternized chitosan
Anion exchange membrane
Fuel cells

ABSTRACT

Novel cross-linked composite membranes were synthesized to investigate their applicability in anion exchange membrane fuel cells. These membranes consist of quaternized poly(vinyl alcohol) (QAPVA) and quaternized chitosan (2-hydroxypropyltrimethyl ammonium chloride chitosan, HACC) with glutaraldehyde as the cross-linking reagent. The membranes were characterized in term of their water content, ion exchange capacity (IEC), ion conductivity and methanol permeability. FTIR, X-ray diffraction and scanning electron microscopy (SEM) were also used to investigate the relation between the structure and performance of the composite membranes. The composite membranes have a high conductivity (10^{-3} to 10^{-2} S cm^{-1}), and a low methanol permeability (from 5.68×10^{-7} to 4.42×10^{-6} cm^2 s^{-1}) at 30 °C. After reviewing all pertinent characteristics of the membranes, we find that the membrane structure is the principal factor affecting the conductivity and methanol permeability of these membranes.

1. Introduction

It is commonly believed that polymer electrolyte membrane fuel cells are destined to become an effective energy alternative [1,2]. Among the various fuel cell technologies, the direct methanol fuel cell (DMFC) holds favor as a promising candidate for its application as a portable power source, owing to its ease of storage and use of methanol as a liquid fuel. DMFCs use currently proton exchange membranes, such as Nafion®, etc., as a barrier to separate the fuel and to transport protons. These membranes can provide high proton conductivity and cell power, but with low methanol barriers, which results in power losses [3,4]. Consequently, alkaline anion exchange membrane fuel cells (AEMFCs) have been developed to avoid the deficiencies of DMFCs containing proton exchange membranes. Because the operational environment is alkaline, AEMFCs have many advantages, including: (1) the methanol oxidation rate is faster in alkaline media than in acid [5]; (2) AEMFCs can use less expensive metal catalysts, such as Ag or Ni; (3) the direction of OH^- anion motion opposes that of the methanol flux through the membrane leading to an intrinsic reduction in methanol permeability.

Research on the application of anion exchange membranes has been underway for several years [6–12]. There are many ways to produce anion exchange membranes, such as radiation grafting, electrophilic substitution or dipping with alkali metal hydroxide, such as KOH. (2,3-Epoxypropyl) trimethylammonium chloride (EPTMAC) is an active electrophilic reagent that can react with —OH or $-NH_2$ groups and hence graft quaternary ammonium groups onto the polymer matrix [13,14]. Therefore, this electrophilic reaction with EPTMAC can be used to synthesize anion exchange membranes. In our previous work, we have investigated quaternized poly(vinyl alcohol) (QAPVA) obtained by the reaction between PVA and EPTMAC and have produced cross-linked QAPVA membranes, which have good conductivity and low methanol permeability [8].

Cross-linked QAPVA membranes have a weak mechanical strength. Their performance can be improved by several means, such as blending with inorganic materials or other polymers. The objective of this work is to blend QAPVA with other materials to produce a composite membrane that has a more compact structure and good mechanical strength.

Chitosan (CS), which has a low toxicity and is biodegradable and biocompatible, is one of the most abundant natural polymers from the ocean. CS has been studied as a membrane material for ultrafiltration, reverse osmosis, pervaporation and fuel cells [15–17]. Because there are no mobile hydrogen ions in its structure, CS has a low electrical conductivity. Quaternized CS (2-hydroxypropyltrimethyl ammonium chloride chitosan, HACC), the product of the reaction of CS and EPTMAC, has exchangeable OH^- anions arising from the quaternary ammonium groups in the matrix. HACC has been used as a flocculant in water treatment [18,19] and is also used as a membrane material for electrolyte separation and pervaporation [20,21]. However, it has not been used in fuel cells.

* Corresponding author. Tel.: +86 592 2183751; fax: +86 592 2184822.
E-mail address: qlliu@xmu.edu.cn (Q.L. Liu).

0378-7753/$ – see front matter © 2008 Elsevier B.V. All rights reserved.
doi:10.1016/j.jpowsour.2008.06.004

Table 1
The characteristics and activation energies (E_a) of the composite membranes

Membrane	P4H1G2	P4H1G4	P4H1G8	P3H2G2	P3H2G4	P3H2G8
QAPVA (wt%)	4	4	4	3	3	3
HACC (wt%)	1	1	1	2	2	2
10 wt% GA (mL)[a]	0.2	0.4	0.8	0.2	0.4	0.8
E_a (kJ mol^{-1})	11.8	16.7	14.4	15.6	13.5	17.9

[a] The quantity of GA is added in a 20-mL composite solution.

Considering the anion exchange groups in HACC, it should be possible to apply HACC in alkaline anion exchange membrane fuel cells.

HACC is a good choice for AEMFCs, since it has —OH and —NH_2 groups that can react with glutaraldehyde (GA) to form a cross-linking network, which reinforces the strength of the membrane [17]. It also has quaternary ammonium groups and exchangeable OH^- anions. When HACC is added into the membranes, its exchangeable groups can improve the ion conductivity of the composite membranes.

According to its good performance and low cost as noted above, HACC was chosen as the polymer material to blend with QAPVA to produce anion exchange membranes for application in alkaline fuel cells. In this paper, we prepared cross-linked QAPVA and HACC composite membranes and assessed their characteristics.

2. Experimental

2.1. Material and membrane preparation

Poly(vinyl alcohol) (polymerization degree of 2400, hydrolysis degree of 98–99%) was supplied by Sinopharm Chemical Reagent Co. Ltd. Chitosan has a degree of deacetylation of approximately 92% (Yuhuan Ocean Biochemical Co. Ltd., China). EPTMAC (purity ≥95%) was purchased from Shandong Guofeng Fine Chemistry Factory. Quaternized poly(vinyl alcohol) was synthesized according to the previously reported study [8]. 2-Hydroxy-propyltrimethy ammonium chloride chitosan was synthesized according to the method reported by Lin et al. [22]. Glutaraldehyde (25 wt% content in distilled water) was supplied by Sinopharm Chemical Reagent Co. Ltd.

QAPVA and HACC were dissolved in deionized water to obtain a solution with a total concentration of 5 wt%. The pH of the solution was adjusted to 5 with 10 wt% sulfuric acid. Then a quantitative amount of 10 wt% GA was added as a cross-linking reagent. After the above solution was filtered with a G3 sand filter, it was coated onto the surface of a glass plate and dried at 45 °C for 6 h. The membrane was removed from the glass plate and dried at 100 °C for 3 h.

Two series of composite membranes were prepared and their characteristics were contrasted as shown in Table 1. The following codes were used to name these composite membranes: P means QAPVA, H means HACC and G means GA. The number behind each letter indicates the weight percent of each composition, except for GA, where the number indicates the number of mL of GA added in a 20-mL mixture to prepare a given membrane. For example, P3H2G2 means that in this membrane the concentration of QAPVA is 3 wt% that of HACC is 2 wt% and the amount of GA added per 20 mL of mixture is 2 mL.

2.2. Structural characterization

The FT-IR absorption spectra of CS, HACC, QAPVA and the composite membranes were recorded using an FT-IR740SX spectrophotometer (Thermo Electron Corporation, USA). The crystal structures of the composite membranes were examined using an X-ray diffractometer (X'Pert Pro, Panalytical, Holland). Also the membrane samples were scanned in the reflection mode with a 2θ angle between 5° and 35°. TGA thermal analyses were carried out using a TG209F1 (NETZSCH, Germany) system. The measurements were conducted by heating from 30 to 600 °C at a heating rate of 10 °C min^{-1} under a nitrogen atmosphere.

The membrane morphologies were investigated by environment scanning electron microscopy (XL30ESEM-TMP, Philips, Holland). Prior to observations, the membrane samples were fractured in liquid nitrogen and then sputtered with gold.

2.3. Water content and ion exchange capacity (IEC)

Water content studies of the composite membranes were carried out by measuring the change in weight of the composite membranes before and after hydration using an electronic scale (AR3130, Ohaus Corporation, USA). The OH^- form composite membranes were immersed in deionized water at room temperature and equilibrated for more than 48 h. The weight of the wet composite membrane was determined after removing excess surface water. Then the wet membrane was dried under vacuum at a fixed temperature of 60 °C until a constant dry weight was obtained. The percentage water content W_c was calculated using the following relation:

$$W_c\ (\%) = \frac{m_h - m_d}{m_d} \times 100 \quad (1)$$

where m_h is the mass (g) of a wet membrane and m_d is the mass (g) of a dry membrane.

The ion exchange capacity was measured using the classical titration method. The composite membranes were soaked in a large volume of 0.1 M NaOH solution to convert them into the OH^- form. They were washed with deionized water to remove excess NaOH and then equilibrated with 100 mL of 0.1 M HCl solution for 48 h. The IEC values were determined from the reduction in acid measured using back titration. The IEC values (mequiv. g^{-1}) were obtained from the following equation:

$$\text{IEC}\ (\text{mequiv.}\,\text{g}^{-1}) = \frac{M_{o,HCl} - M_{e,HCl}}{m_d} \quad (2)$$

where $M_{o,HCl}$ is the milliequivalents (mequiv.) of HCl required before equilibrium, $M_{e,HCl}$ is mequiv. of HCl required after equilibrium, and m_d is the mass (g) of the dried membrane.

2.4. Methanol permeability

The methanol permeability was measured using a diffusion cell comprising two compartments. Magnetic stirrers were used in each compartment to ensure uniformity during the experiments. The membrane was clamped between the two compartments. One compartment was loaded with deionized water and the other with a solution containing 1 M methanol and 0.5 M KOH. The concentration of the permeating methanol was measured by gas chromatography (GC-950, Shanghai Haixin Chromatographic Instruments Co., Ltd.).

2.5. Ion conductivity

The ion conductivity of the membranes was measured by two-probe AC impedance spectroscopy with Parstat 2273 electrochemical equipment (Princeton Advanced Technology, USA) over the frequency range from 0.1 to 1 MHz. Before testing, the OH^- form membranes were hydrated in deionized water for at least 48 h. The testing device with the membrane was placed in a chamber with deionized water to keep the relative humidity at 100% during the measurements.

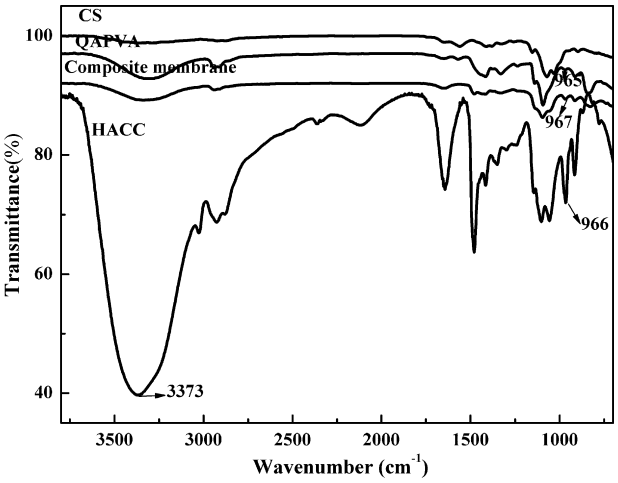

Fig. 1. FT-IR spectra of CS, QAPVA, HACC and composite membranes.

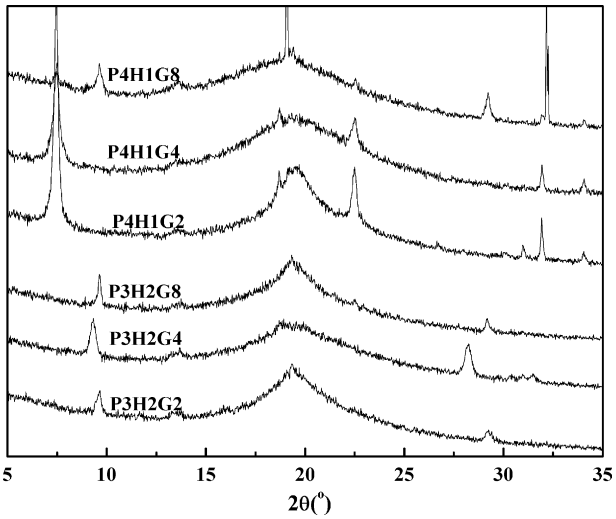

Fig. 2. XRD patterns of the composite membranes.

The ion conductivity σ (S cm^{-1}) of a given membrane can be calculated from

$$\sigma = \frac{l}{R \times A} \quad (3)$$

where l is the distance (cm) between two stainless steel electrodes, A is the cross-sectional area (cm^2) of the membrane and R is the membrane resistance (Ω) from the AC impedance data.

3. Results and discussion

3.1. FTIR-ART spectroscopy

IR spectra were determined to assess the existence of —OH groups in the membranes. The IR spectra of QAPVA, HACC and the composite membranes are shown in Fig. 1. The peaks at 965, 966 and 967 cm^{-1}, found in the IR spectra of QAPVA, HACC and the composite membranes, respectively, are characteristic absorptions of quaternary ammonium groups. But the same peak does not show in the IR spectra of CS. This indicates that quaternary ammonium groups have been introduced to CS successfully.

The IR spectrum of the cross-linked composite membrane shows a decrease in the intensity of the O—H band (3200–3500 cm^{-1}) compared to that of HACC, which arises from the cross-linking reaction. The composite of QAPVA and HACC can be cross-linked by GA through the reaction of —OH with —C═O groups.

3.2. XRD analysis

The X-ray diffraction measurements were performed to examine the crystallinity of the composite membranes. PVA and CS are well known to exhibit a semi-crystalline structure. The introduction of quaternary ammonium groups disrupts the crystalline structure of the polymers; therefore, QAPVA and HACC have a low crystallinity. Fig. 2 shows the XRD patterns of two series of composite membranes. From the patterns, the P3H2 series shows a large peak at the 2θ angle of 18–20° and a small peak at 9–10°. The large peak at 2θ = 18–20° for the P3H2G4 membrane is broadened compared to that for the P3H2G2 membrane, which indicates a decrease of the crystalline area in the composite membranes. The crystallinity of the composite membranes is due to the hydroxyl groups in the side-chain of QAPVA and HACC, which forms intramolecular hydrogen bonds and hence crystalline areas. With the addition of GA, the cross-linking reaction between the —OH groups on HACC and QAPVA and the —C═O groups on GA occurs and weakens the intramolecular hydrogen bonds. This leads to a decrease in the crystallinity of the composite membranes. However the large peak at 2θ = 18–20° for the P3H2G8 membrane does not change significantly. The cross-linking makes the structure of the membranes compact and generates new crystalline areas. Intramolecular hydrogen bonds breaking and the generation of new crystalline areas caused by cross-linking work in opposite directions, so that the crytallinity of the P3H2G8 membrane changes little.

Fig. 2 also illustrates the diffraction patterns of the P4H1 series of composite membranes. With the addition of GA, the peak at 2θ = 18–20° is broadened. The effect of breakage of the intramolecular hydrogen bonds plays a dominant role, accordingly the crystallinity of P4H1 series of composite membranes decreases with increasing GA content.

Comparing the XRD patterns of the P3H2 and the P4H1 series of composite membranes, we find that the peak intensity of the latter is weaker than that of the former, with the same amount of cross-linking reagent. This tendency shows that the crystallinity of the P4H1 series of membranes is less than that of the P3H2 series. The ion conductivity of the composite membranes is related to the crystallinity. A high crystallinity discourages the transport of ions in the membrane. Consequently the P4H1 series of composite membranes have better ion conductivity than those of the P3H2 series (the results are given in Section 3.6).

3.3. TGA thermal analysis

Fig. 3 shows the TGA and differential gravimetric analysis (DTG) thermographs of the QAPVA membrane, which reveal three principal weight loss regions and three peaks in the DTG curves. The first peak transition region (around 298 °C) arises from the degradation of the quaternary ammonium groups grafted onto the matrix; the total weight loss at this stage is about 42%. The second peak transition region at 352 °C arises from the degradation of hydroxyl groups on the matrix; the total weight loss corresponding to this stage is about 40%. The third peak at 426.5 °C leads to the cleavage of the backbone of the QAPVA; the total weight loss here is about 99% at 566 °C.

Fig. 4 shows the TGA and DTG thermographs of HACC. The curves reveal one principal weight loss region, and there exists one peak in the DTG curve. The main transition region at 230–280 °C (T_{max} = 258 °C) arises from the degradation of the quaternary

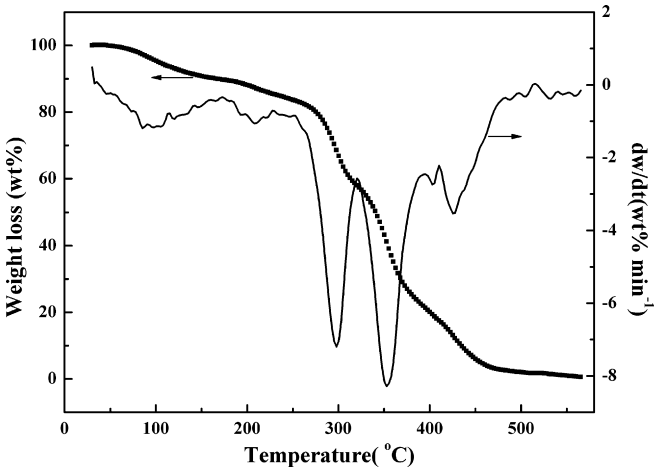

Fig. 3. TGA curve of the QAPVA membranes.

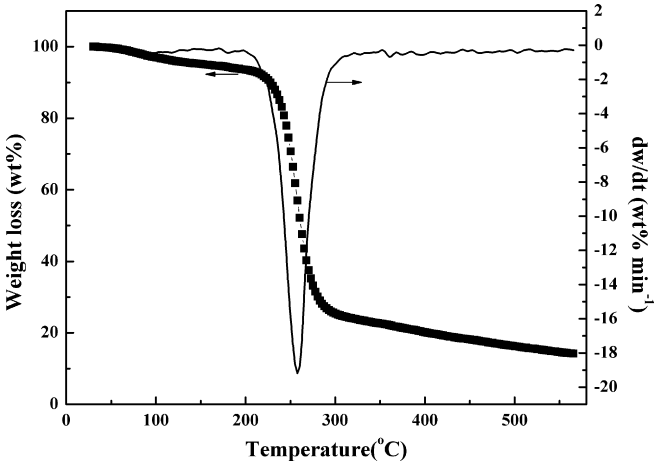

Fig. 4. TGA curve of the HACC membranes.

ammonium groups on the chain and the cleavage of the backbone of HACC; the total weight loss is about 86% at 566 °C. This result suggests that the bonds of 2-hydroxy-propyltrimethy ammonium groups and the NH— linkage are very stable.

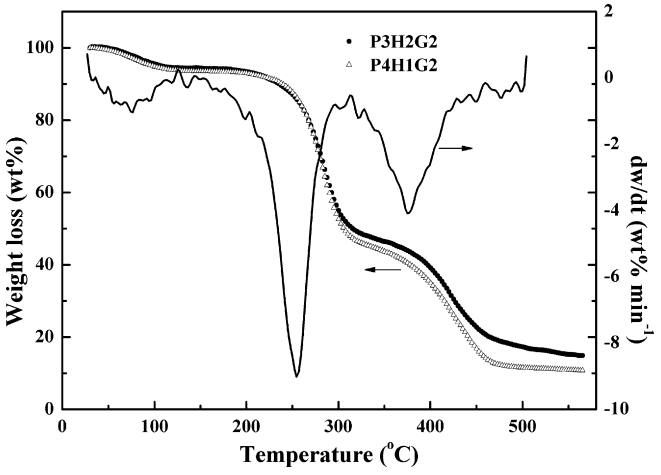

Fig. 5. TGA curve of the P3H2G2 and P4H1G2 composite membranes.

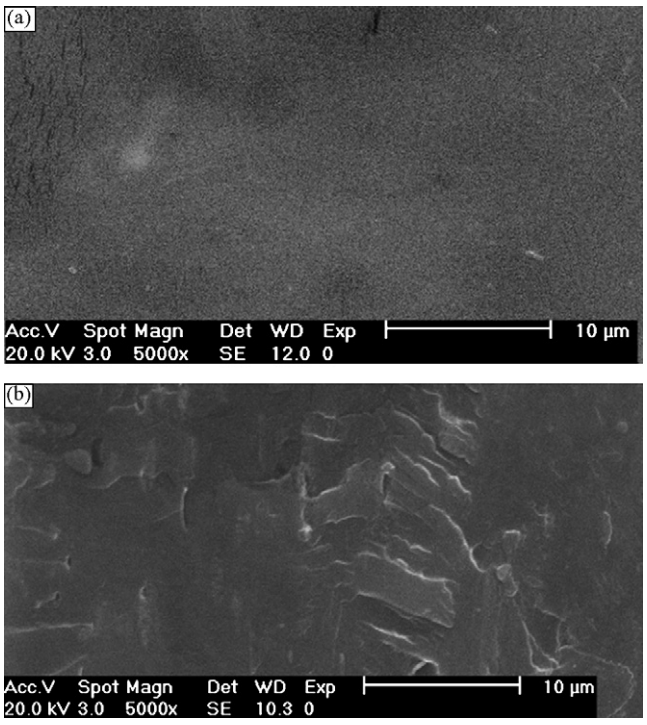

Fig. 6. SEM photographs of the P3H2G4 composite membrane: (a) surface image and (b) cross-sectional image.

Fig. 5 shows the TGA and DTG thermographs of the P3H2G2 cross-linked composite membrane. There are two principal weight loss regions and two peaks in the DTG curve. The first peak transition region at 285 °C arises from the degradation of quaternary ammonium groups; the weight loss corresponding to this stage is about 54%. The second stage at 360–420 °C (T_{max} = 421.1 °C) arises from the cleavage of the C–C backbone of the composite membranes, and the total weight loss here is about 85% at 566 °C. Note the TGA curve of P4H1G2 membrane in Fig. 5. A comparison of the TGA curves of the P3H2G2 and P4H1G2 membranes reveals that the degradation trends of the two membranes are almost the same. Also the P3H2G2 membrane is somewhat more stable than the P4H1G2 membrane, which is due to the variable content of QAPVA and HACC. The degradation of the composite membrane P3H2G2 is less intense than that of the QAPVA and HACC membranes, which is due to the cross-linked network formed in the composite membranes. Hence, the content of QAPVA and HACC and the cross-linking degree determine the mechanical stability of the composite membranes.

3.4. Scanning electron microscopy (SEM)

SEM photographs for the surface and the cross-sectional views of the P3H2G4 composite membrane are shown in Fig. 6. The surface of the composite membrane is smooth. And the cross-sectional view of the composite membrane shows that there are no obvious holes, phase separation phenomena and the structure is compact. The results indicate that QAPVA and HACC are combined well with GA as the cross-linking reagent.

3.5. Water content and ion exchange capacity (IEC)

Fig. 7 shows the water content of the composite membranes, which is found to decrease with increasing GA addition for all composite membranes. This arises from the formation of cross-

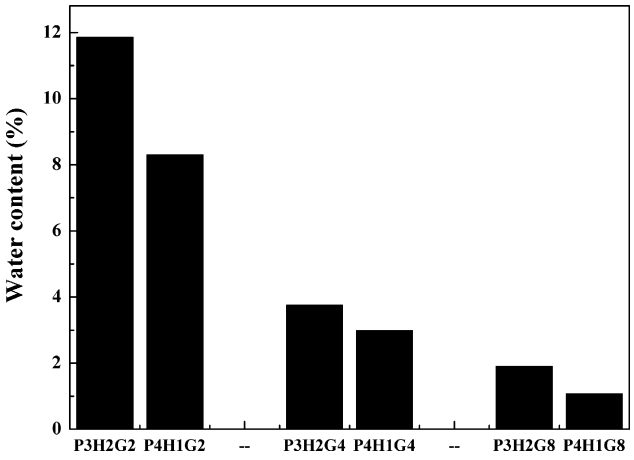

Fig. 7. Water content of the composite membranes.

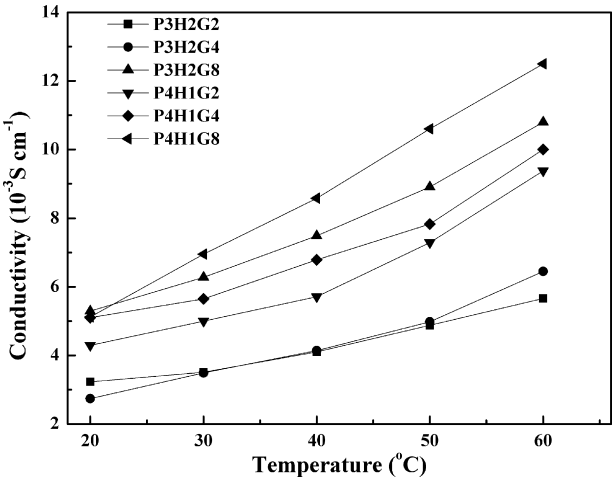

Fig. 9. Ion conductivity of the composite membranes.

linked structures, which become more compact with more GA as the cross-linking reagent. Hence, there is not much space in the composite membranes to contain water molecules.

The water content of the P3H2 series of membranes is greater than that of the P4H1 series, when they have the same volume of GA as the cross-linking reagent. The different quantity of QAPVA and HACC in the membranes results in different water content. This result indicates that the HACC membrane is more hydrophilic than the QAPVA membrane. The former can contain more water molecules than the latter with the same mass.

The ion exchange capacity (IEC) indicates the intensity of exchangeable hydrophilic groups grafted onto the membrane matrix, which is responsible for their charged nature. Fig. 8 shows the ion exchange capacity of the composite membranes. It can be seen that the IEC of the P3H2 series of membranes is greater than that of the P4H1 series because of the increasing number of charged groups ($-N^{+}(CH_3)_3$) in the P3H2 series. This result indicates that the number of charged groups per gram of QAPVA is larger than that in HACC.

3.6. Ion conductivity

Fig. 9 shows the conductivity of all the composite membranes as a function of temperature. The conductivities of all the membranes range from 10^{-3} to 10^{-2} S cm^{-1}, with the highest being 1.25×10^{-2} S cm^{-1} at 60 °C for the P4H1G8 membrane, which is higher than that of the cross-linked QAPVA membranes (8.37×10^{-3} S cm^{-1}) at the same temperature [8].

The conductivity of the P4H1 series of membranes is higher than that of the P3H2 series with the same mass of GA. This result is the reverse to the common assumption that the IEC and the water content control the ion conductivity. The IEC and water content of the P3H2 series of membranes are higher than those of the P4H1 series. The higher IEC means more charged groups, and the higher water content means more water in the membranes. But the conductivity results reveal that an increase of the IEC of these composite membranes is not the primary determining factor for the ion conductivity. The water in the membranes exists in two forms: free water and bound water. The water content is the total of the free and bound water, whereas only the free water can transport OH^- groups through the membrane. Hence, we presume that the free water content in the P4H1 series of membranes is greater than that in the P3H2 series, which also affects the conductivity of the composite membranes.

As shown in Fig. 9, the ion conductivity of the same series composite membrane increases with increasing cross-link density and decreasing water content of the membranes. This phenomenon is different from other cross-linked membranes [23,24] and can be explained by structural effect as indicated from the XRD results. The transport of OH^- anions in membranes is affected by the water content and the microscopic membrane channel structure. The XRD plot shows that the P4H1 series of membranes have fewer crystalline regions than those of the P3H2 series, so it is easier to form run-through anion transport channels in the P4H1 series than in the P3H2 series. Hence, the transport of OH^- anions is easier in the P4H1 series membranes than in the P3H2 series. All these results indicate that the membrane structure is the dominant factor in determining the facility of anion transport in these composite membranes.

These membranes, which have a high conductivity and low water content, can achieve almost perfect performance as described by Anis et al. [23].

Fig. 10 shows the relation between $\ln\sigma$ and $1000/T$. Assuming that the conductivity follows the Arrhenius behavior, the ion transport activation energy E_a of the composite membranes can be obtained according to the Arrhenius equation:

$$E_a = -b \times R \quad (4)$$

where b is the slope of the regression line of $\ln\sigma$ (S cm^{-1}) vs. $1000/T$ (K^{-1}) plots and R is the gas constant (8.314472 J K^{-1} mol^{-1}). The

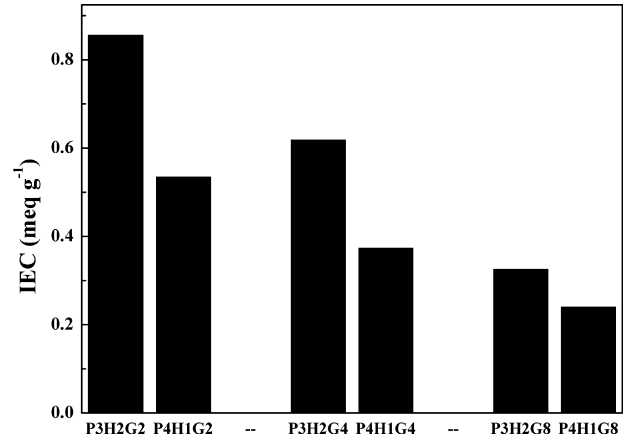

Fig. 8. Ion exchange capacity of the composite membranes.

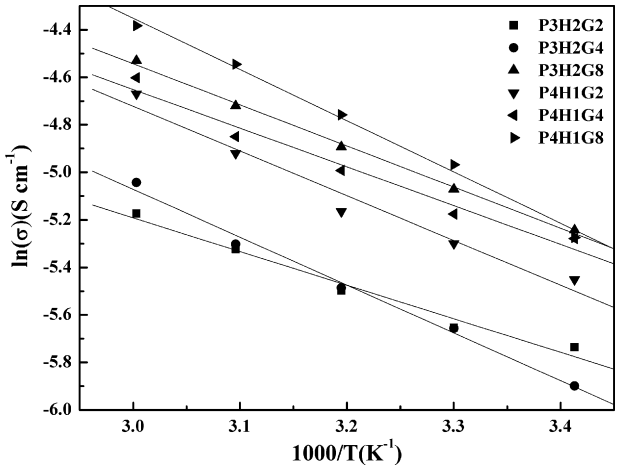

Fig. 10. Arrhenius plots for the composite membranes.

results are presented in Table 1. The E_a of the P4H1G2 membranes (11.8 kJ mol^{-1}) is the lowest of all the composite membranes.

The E_a values of the cross-linked QAPVA membranes [8] and the cross-linked PVA/PAA/silica hybrid membranes [25] increase with increasing cross-linking degree. However, the E_a values of the QAPVA/HACC composite membranes change in a different manner. Here, in the same series of membranes, the E_a values do not increase with increasing cross-linking degree. Between the two series membranes, the E_a values change without any discernable pattern. The composition and the structure of the membranes are two factors that influence the value of E_a. Based on the E_a values of the composite membranes; it is possible that the combined effect of the composition and structure determines the E_a values of the composite membranes. Consequently, the E_a values of these membranes show a random distribution.

3.7. Methanol permeability

The methanol permeability of all the cross-linked composite membranes as a function of temperature is shown in Fig. 11. The methanol permeability ranges from 5.68×10^{-7} to 4.42×10^{-6} cm^2 s^{-1} at 30 °C with 1 M methanol in one compartment. These values are smaller than those of the cross-linked QAPVA membranes [$(1.0–4.1) \times 10^{-6}$ cm^2 s^{-1}] [8] and Nafion® 117 membranes [$(4.5–9.2) \times 10^{-6}$ cm^2 s^{-1}] [16]. At the same time, it is also observed that the methanol permeability increases only slightly with increasing temperature. For example, for the P4H1G8 membranes, their methanol permeabilities are 1.42×10^{-6}, 0.95×10^{-6}, 1.42×10^{-6} and 1.89×10^{-6} cm^2 s^{-1} at 30, 40, 50 and 60 °C, respectively. These data indicate that the cross-linked composite membranes have low methanol permeability and hence can be applied to better advantage in anion exchange membrane fuel cells.

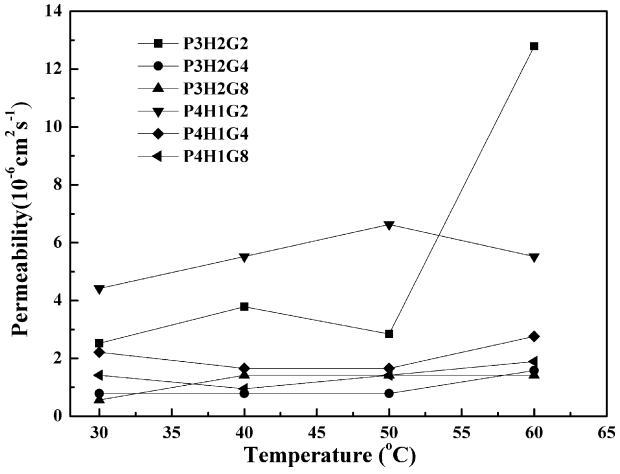

Fig. 11. Methanol permeability of the composite membranes.

The methanol permeability of these two series of membranes also decreases with increasing GA, which can be explained by the fact that the addition of GA forms a more compact structure in the cross-linked composite membranes. The more compact structure makes the transport channels narrower; hence, it increases the transport resistance for methanol passing through the cross-linked composite membranes.

4. Conclusions

Two series of novel cross-linked composite anion exchange membranes were prepared using different mass of QAPVA and HACC and using GA as the cross-linking reagent. With the quaternary ammonium group grafted onto the matrix of QAPVA and HACC, the composite membranes have exchangeable anions. Also the form of the cross-linking structure reduces the methanol permeability of the composite membranes. The composite membranes show high conductivity in the range of 10^{-3} to 10^{-2} S cm^{-1} and low methanol permeability. It is found that the membrane structure is the principal factor affecting the conductivity and methanol permeability of the composite membranes.

Acknowledgements

The support of National Nature Science Foundation of China Grant no. 50573063, the Program for New Century Excellent Talents in University and the research fund for the Doctoral Program of Higher Education (no. 2005038401) in preparation of this article are gratefully acknowledged. The authors gratefully acknowledge Professor Sun shigang and his Research Group for their kind help. The authors are grateful to Prof. James R. Bolton from the Department of Civil and Environmental Engineering at the University of Alberta for his kind assistance with our English writing.

References

[1] H. Voss, J. Huff, J. Power Sources 65 (1997) 155–158.
[2] C.K. Dyer, J. Power Sources 106 (2002) 313–322.
[3] H. Nitani, T. Nakagawa, H. Daimon, Y. Kurobe, T. Ono, Y. Honda, A. Koizumi, S. Seino, T.A. Yamamoto, Appl. Catal. A: Gen. 326 (2007) 194–201.
[4] J.S. Wang, X.Z. Deng, J.Y. Xi, L.Q. Chen, W.T. Zhu, X.P. Qiu, J. Power Sources 170 (2007) 297–302.
[5] Y. Wang, L. Li, L. Hu, L. Zhuang, J.T. Lu, B.Q. Xu, Electrochem. Commun. 5 (2003) 662–666.
[6] T.N. Danks, R.C.T. Slade, J.R. Varcoe, J. Mater. Chem. 13 (2003) 712–721.
[7] J.R. Varcoe, R.C.T. Slade, Electrochem. Commun. 8 (2006) 839–843.
[8] Y. Xiong, J. Fang, Q.H. Zeng, Q.L. Liu, J. Membr. Sci. 311 (2008) 319–325.
[9] L. Lei, Y.X. Wang, J. Membr. Sci. 262 (2005) 1–4.
[10] C.C. Yang, S.J. Lin, G.M. Wu, Mater. Chem. Phys. 92 (2005) 251–255.
[11] J. Fang, P.K. Shen, J. Membr. Sci. 285 (2006) 317–322.
[12] Y. Wan, B. Peppley, K.A.M. Creber, V.T. Bui, E. Halliop, J. Power Sources 162 (2006) 105–113.
[13] H. Touzi, N. Sakly, R. Kalfat, H. Sfihi, N. Jaffrezic-Renault, M.B. Rammah, H. Zarrouk, Sens. Actuator B: Chem. 96 (2003) 399–466.
[14] P.R. Meng, L.B. Li, H.X. Qin, X.C. Liu, C.X. Chen, J. Chem. Ind. Eng. (China) 57 (2006) 1718–1721.
[15] C.X. Liu, R.B. Bai, J. Membr. Sci. 284 (2006) 313–322.
[16] J.H. Chen, Q.L. Liu, J. Fang, A.M. Zhu, Q.G. Zhang, J. Colloid Interface Sci. 316 (2007) 580–588.
[17] B. Smitha, S. Sridhar, A.A. Khan, J. Power Sources 159 (2006) 846–854.
[18] W.M. Cai, Y. Ye, P.X. Chen, Environ. Pollut. Control. 21 (1999) 1–4.
[19] Z.S. Cai, Z.Q. Song, S.B. Shang, C.S. Yang, Polym. Bull. 59 (2007) 655–665.

[20] R.H. Huang, G.H. Chen, M.K. Sun, Y.M. Hu, C.J. Gao, Carbohydr. Polym. 70 (2007) 318–323.
[21] A. Saxena, A. Kumar, V.K. Shali, J. Colloid Interface Sci. 303 (2006) 484–493.
[22] Y.W. Lin, Q. Lin, Z.Q. Jiang, W.C. Zhang, C. Xu, Chin. J. Appl. Chem. 19 (2002) 351–354.
[23] A. Anis, A.K. Banthia, S. Bandyopadhyay, J. Power Sources 179 (2008) 69–80.
[24] I.Y. Jang, O.H. Kweon, K.E. Kim, G.J. Hwang, S.B. Moon, A.S. Kang, J. Power Sources 181 (2008) 127–134.
[25] D.S. Kim, H.B. Park, J.W. Rhim, Y.M. Lee, Solid State Ionics 176 (2005) 117–126.